

Fast Cleavage Reactions following Electron Transfer. Reduction of 1,1-Dinitrocyclohexane

Janet C. Rühl,^{1a} Dennis H. Evans,^{*1a} Philippe Hapiot,^{1b} and Pedatsur Neta^{1b}

Contribution from the Department of Chemistry and Biochemistry, University of Delaware, Newark, Delaware 19716, and Chemical Kinetics Division, National Institute of Standards and Technology, Gaithersburg, Maryland 20899. Received February 11, 1991

Abstract: One-electron reduction of 1,1-dinitrocyclohexane is followed by rapid cleavage of a C-N bond, giving nitrite and 1-nitrocyclohexyl radical. The rate constant has been determined in dimethylformamide by homogeneous redox catalysis ($1.6 \times 10^6 \text{ s}^{-1}$) and in aqueous solution by pulse radiolysis ($1.1 \times 10^6 \text{ s}^{-1}$). These values are of the order of 10^6 larger than the rate constant for cleavage of mononitroalkane radical anions. In the case of electrochemical reduction, the electron transfer and bond cleavage are followed by further reduction of the nitroalkyl radical to give the nitronate anion of nitrocyclohexane. For scan rates exceeding about 0.1 V/s in cyclic voltammetry, the 1-nitrocyclohexyl radical is reduced by the anion radical of 1,1-dinitrocyclohexane rather than at the electrode. Controlled potential electrolysis and product analysis showed that about 1.2 electrons were required per molecule of 1,1-dinitrocyclohexane; essentially no nitronate was found, but instead some nitrocyclohexane and substantial amounts of 1,1'-dinitrobicyclohexyl (**5**) were produced. This latter product arises from the radical chain reaction of nitronate with starting material. A key chain-carrying step in this reaction scheme is the reaction of 1-nitrocyclohexyl radical with the nitronate to give the anion radical of **5**. The rate constant for this step was found to be $2.6 \times 10^6 \text{ L mol}^{-1} \text{ s}^{-1}$ in water by pulse radiolysis. Fitting of fast-scan cyclic voltammograms by digital simulation showed that this rate constant must be about $5 \times 10^8 \text{ L mol}^{-1} \text{ s}^{-1}$ in dimethylformamide with a termination reaction ($k_t = 2 \times 10^4 \text{ s}^{-1}$) of hydrogen atom abstraction by 1-nitrocyclohexyl to produce the nitrocyclohexane found in the electrolyzed solutions.

The early stages of the reduction of many organic compounds involve the transfer of an electron to the reactant followed by bond cleavage, freeing an atom or other leaving group. In some cases, most notably the reduction of alkyl halides, the radical anion may not exist as a true intermediate, the alkyl radical and halide being formed in a single-step "dissociative electron-transfer" reaction.² In other instances, the radical anions enjoy a brief but measurable lifetime before cleavage occurs.

Aliphatic nitro compounds provide a good illustration of the effect of structure on the rate of the cleavage reaction. The most carefully studied examples involve cleavage of the C-N bond from a tertiary carbon center, giving an alkyl radical and nitrite,³ where it has been found that the rate constant for the cleavage reaction increases about 3 orders of magnitude on going from a mononitroalkane to a *vic*-dinitro compound. In the present work, we have found an additional increase of 3 orders of magnitude for a *gem*-dinitro compound, 1,1-dinitrocyclohexane (**1**), whose radical anion has a lifetime of about 1 μs .

Loss of nitrite from the anion radicals of nitro compounds is probably an important step in the synthesis of olefins from *vic*-dinitro compounds,⁴ the reduction of acylated β -nitro alcohols,⁵ and electrochemically induced aromatic substitution using 2-nitropropane anion as nucleophile.⁶ For *gem*-dinitro compounds specifically, this rapid cleavage reaction is a key step in the radical chain reactions of these compounds with a host of nucleophiles.⁷

In the present paper, the reduction of **1** has been investigated by voltammetric techniques and by pulse radiolysis. The rate of the cleavage reaction has been determined as well as that of a subsequent step in the overall process. The resulting analysis constitutes the first quantitative depiction of an electrochemical reduction reaction followed by a radical chain process.

Experimental Section

Reagents. Dimethyl sulfoxide (DMSO) was from Aldrich, and *N,N*-dimethylformamide (DMF) was obtained from a number of suppliers (Fisher, Baker (analyzed), Aldrich (Sure-Seal), Burdick and Jackson (high purity)). DMF was stored under nitrogen, and both DMF and DMSO were passed through a column of activated alumina (activated under nitrogen at 400 °C for at least 24 h) just before use. Benzonitrile (Fisher) was dried over CaSO_4 overnight, distilled from CaSO_4 , and then distilled twice from P_2O_5 . It was stored under nitrogen and used directly. Tetra-*n*-butylammonium hexafluorophosphate (TBAPF₆) was obtained from Aldrich, recrystallized three times from ethanol, vacuum dried at 120 °C for at least 18 h, and stored in a desiccator.

1,1-Dinitrocyclohexane⁸ (**1**) and 1,1'-dinitrobicyclohexyl⁹ (**5**) were prepared according to the literature. Nitrocyclohexane, 2-nitrobenzonitrile, and di-*tert*-butyl nitroxide (Aldrich) were used as received.

Water for the pulse radiolysis experiments was purified by a Millipore Super-Q system. The alcohols *tert*-butyl alcohol and isopropyl alcohol were analytical reagents from Mallinckrodt.

Electrochemical Instrumentation. Instrumentation and procedures for cyclic voltammetry, including the construction of microelectrodes and reference electrodes, has been described in earlier publications.^{3a,10,11} The silver reference electrode (AgRE) was composed of a silver wire in contact with 0.010 M AgNO_3 , 0.10 M TBAPF₆, and DMF. Controlled potential coulometry was carried out in a 15-mL cell with a ca. 30 cm² platinum gauze cathode. The auxiliary electrode (platinum wire) compartment was separated from the working electrode compartment by two medium-porosity glass frits.

Pulse Radiolysis. These experiments utilized 50-ns pulses of 2-MeV electrons from a Febetron 705 pulser.¹² The kinetic spectrophotometric

(1) (a) University of Delaware. (b) National Institute of Standards and Technology.

(2) (a) Andrieux, C. P.; Gallardo, I.; Savéant, J.-M.; Su, K.-B. *J. Am. Chem. Soc.* **1986**, *108*, 638-647. (b) Savéant, J.-M. *J. Am. Chem. Soc.* **1987**, *109*, 6788-6795. (c) Andrieux, C. P.; Gallardo, I.; Savéant, J.-M. *J. Am. Chem. Soc.* **1989**, *111*, 1620-1626.

(3) (a) Hoffmann, A. K.; Hodgson, W. G.; Jura, W. H. *J. Am. Chem. Soc.* **1961**, *83*, 4675-4676. (b) Hoffmann, A. K.; Hodgson, W. G.; Maricle, D. L.; Jura, W. H. *J. Am. Chem. Soc.* **1964**, *86*, 631-639. (c) Bowyer, W. J.; Evans, D. H. *J. Org. Chem.* **1988**, *53*, 5234-5239.

(4) (a) Kornblum, N.; Boyd, S. D.; Pinnick, H. W.; Smith, R. G. *J. Am. Chem. Soc.* **1971**, *93*, 4316-4318. (b) Kornblum, N.; Cheng, L. *J. Org. Chem.* **1977**, *42*, 2944-2945. (c) Fukunaga, K.; Kimura, M. *Bull. Chem. Soc. Jpn.* **1979**, *52*, 1107-1111.

(5) Petsom, A.; Lund, H. *Acta Chem. Scand., Ser. B* **1980**, *34*, 614-616.

(6) Amatore, C.; Gareil, M.; Oturan, M. A.; Pinson, J.; Savéant, J.-M.; Thiébaud, A. *J. Org. Chem.* **1986**, *51*, 3757-3761.

(7) (a) Kornblum, N. *Angew. Chem., Int. Ed. Engl.* **1975**, *14*, 734-745. (b) Kornblum, N.; Kelly, W. J.; Kestner, M. M. *J. Org. Chem.* **1985**, *50*, 4720-4724. (c) Russell, G. A. *Prog. Phys. Org. Chem.* **1987**, *23*, 271-322. (d) Russell, G. A.; Baik, W. *J. Chem. Soc., Chem. Commun.* **1988**, 196-198. (e) Bordwell, F. G.; Clemens, A. H. *J. Org. Chem.* **1982**, *47*, 2510-2516. (f) Bordwell, F. G.; Clemens, A. H.; Smith, D. E.; Begemann, J. *J. Org. Chem.* **1985**, *50*, 1151-1156. (g) Bordwell, F. G.; Bausch, M. J. *J. Am. Chem. Soc.* **1986**, *108*, 1985-1988.

(8) Kaplan, R. R.; Schechter, H. J. *J. Am. Chem. Soc.* **1961**, *83*, 3535-3536.

(9) Dornow, A.; Fust, K. *J. Chem. Ber.* **1957**, *90*, 1774-1780.

(10) Bowyer, W. J.; Engelman, E. E.; Evans, D. H. *J. Electroanal. Chem.* **1989**, *262*, 67-82.

(11) Gilicinski, A. G.; Evans, D. H. *J. Electroanal. Chem.* **1989**, *267*, 93-104.

(12) (a) Meot-Ner, M.; Neta, P.; Norris, R. K.; Wilson, K. *J. Phys. Chem.* **1986**, *90*, 168-173. (b) Meot-Ner, M.; Neta, P. *J. Phys. Chem.* **1986**, *90*, 4648-4650. (c) The identification of commercial equipment or material does not imply recognition or endorsement by the National Institute of Standards and Technology, nor does it imply that the material or equipment identified are necessarily the best available for the purpose.

Table I. Controlled Potential Electrolysis^a

solvent	control poten ^c	concn 1 (mM)	n value	% yield ^b		
				dimer 5	nitrocyclohexane (6)	nitrite
DMF	-1.5	3.6	1.2	57	nd ^d	107
	-1.5	4.2	1.1	71	nd	nd
	-1.5	4.4	1.2	48	12	nd
	-1.5	3.8	1.1	51	15	104
	-1.5	10.2 ^e	1.1	51	25	110
DMF + 1% H ₂ O	-1.5	4.1	1.2	55	4	nd
	-1.5	3.9	1.2	44	9	104
Benzonitrile	-1.3	4.1	1.2	40	11	nd
	-1.3	4.1	1.2	47	14	nd
DMF ^f		5.4	1.2	67	nd	91
		5.2	1.2	48	nd	105
DMF ^g		5.2 ^h	1.3	28	34	108

^aElectrolysis of 15 mL of solution at a platinum gauze electrode with 0.10 M TBAPF₆ electrolyte. ^bExpressed as moles of reactant 1 found in products 4, 5, and 6. For nitrite, the yield is based upon 1 mol of nitrite being formed per mole of 1. ^cVolts vs AgRE. ^dNot determined. ^e5% nitronate 4 formed. ^fReduction catalyzed by 1.2 mM 2-nitrobenzonitrile. ^gPlus 0.5 mM di-*tert*-butyl nitroxide. ^h11% nitronate 4 formed.

detection system utilized a 300-W xenon lamp, a Kratos monochromator, an RCA 4840 photomultiplier, and the associated optical components. The signals were digitized with a Tektronix 7612 transient recorder and analyzed with a PC Designs GV-386 computer. The radiation dose ranged from 9 to 20 Gy/pulse, producing between 5 and 12 μM total radical concentrations. Other details of the experiments were as described before.¹²

Analytical Procedures. The determination of nitrocyclohexane by gas chromatography (Varian Model 3700) was carried out by injecting 2-μL samples of the electrolyzed solutions onto a 10% Carbowax 20M Chrom W 60/80, 2 m × 1/8 in. column. The column temperature was 180 °C, and the helium carrier gas flow rate was 30–40 mL/min. Thermal conductivity detection was used (250 °C detector temperature). A working curve (peak height vs concentration) was prepared by using solutions of known concentration of nitrocyclohexane in DMF. Neither 1,1'-dinitrobicyclohexyl nor the electrolyte elute at 180 °C, and it was shown that neither had an effect on the peak height of nitrocyclohexane.

Nitrite was determined by spectrophotometry. A 0.50- or 1.00-mL sample of electrolyzed solution was diluted with water to 100 mL. A 2.00-mL aliquot of this solution was added to 4.00 mL of NEDA-Sulfa solution (5 g of sulfanilamide, 0.25 g of *N*-(1-naphthyl)ethylenediamine dihydrochloride, and 12.5 mL of 85% phosphoric acid made up to 250 mL with water). The color was allowed to develop for 10 min, and the absorbance was determined at 530 nm by using a Bausch and Lomb Spectronic 20 spectrophotometer. A working curve was prepared by using solutions of sodium nitrite (Fisher, oven dried before use) in water containing 1% 0.10 M TBAPF₆/DMF to mimic the composition of the electrolyzed solutions.

Voltammetric studies of the electrolyzed solutions served to identify and to determine the yield of 1,1'-dinitrobicyclohexyl (5) and, in some experiments, to determine the yield of nitrocyclohexane (6). The electrolyzed solutions produced no voltammetric wave for the reactant 1, but 5 and 6 could be detected through their reduction with steady-state half-wave potentials of -1.8 and -2.2 V vs AgRE. Standard addition methods were implemented in the following manner: After the electrolysis, a series of slow-scan (20–100 mV/s) cyclic voltammograms (12.5–50-μm radius platinum disk electrode or mercury-plated 12.5-μm radius platinum disk) was obtained as aliquots of 5 or 6 (10–20 μmol/aliquot) were added to the electrolyzed solutions. Linear plots of peak or limiting currents (depending upon whether steady-state conditions were met) vs amount added were obtained and used to determine the amount of 5 or 6 formed.

Results

General Features of the Electrochemical Reduction of 1. The cyclic voltammogram shown in Figure 1 includes an irreversible reduction peak at -1.4 V followed by a smaller irreversible peak at -2.0 V vs AgRE. On the return sweep, a peak due to oxidation of nitrite (not shown) appears at a variable position, 0.0–0.3 V. No oxidation peak associated with the first reduction peak could be detected at the fastest scan rates and lowest temperature that were practical, 2000 V/s at -50 °C.^{3c} However, the second reduction peak is suppressed at faster scan rates and is scarcely visible under the above conditions. This second peak occurs at the same potential as the peak for the reduction of 5.

Controlled Potential Electrolysis. In order to determine the number of faradays required to reduce 1 mol of reactant (*n* value) as well as the identity and yields of products, controlled potential

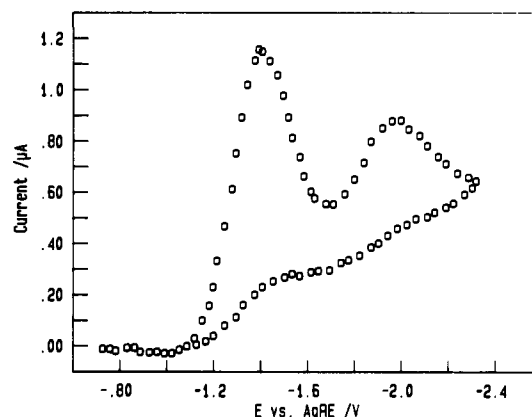
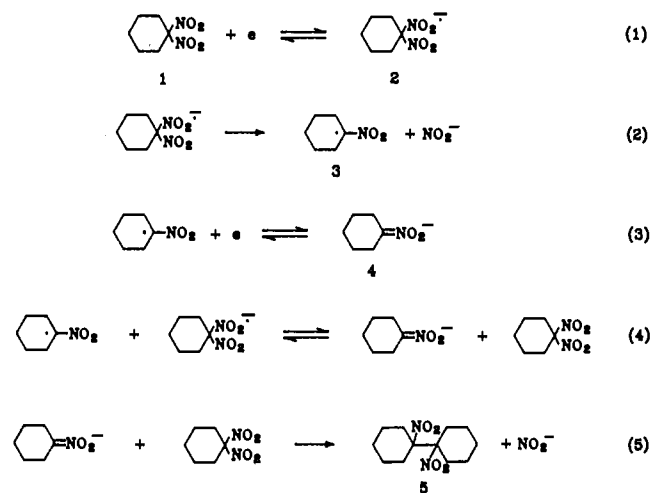


Figure 1. Cyclic voltammogram of 2.4 mM 1,1-dinitrocyclohexane in DMF with 0.10 M TBAPF₆. A 50-μm radius platinum disk working electrode. Scan rate 50 V/s.

Scheme I



electrolyses were performed followed by analysis of the electrolyzed solutions. The results are summarized in Table I.

The principal products are the dimer 5, nitrocyclohexane, and nitrite. Nitronate anion 4 was not present at the end of the electrolysis except when a higher concentration of 1 was electrolyzed, 10 mM. A reasonable working hypothesis for the first steps of the reduction is the sequence given by eqs 1–4 (Scheme I) in which the postulated anion radical 2 is a short-lived intermediate. The dimer 5 could be derived from dimerization of nitroalkyl radical 3 or by the follow-up reaction of 4 with starting material by overall eq 5, a known reaction that occurs by a radical chain process.^{7a,13} If eqs 1–5 accounted for the entire reaction,

Table II. Homogeneous Redox Catalysis of the Reduction of 1,1-Dinitrocyclohexane Using 2-Chloro-9,10-anthraquinone as Catalyst^a

C_P^* (mM)	v (V/s)	$\gamma = 1.0$			$\gamma = 2.0$			$\gamma = 4.0$		
		i_p/i_{pd}	$\log k_6^b$	$\log k_6^c$	i_p/i_{pd}	$\log k_6^b$	$\log k_6^c$	i_p/i_{pd}	$\log k_6^b$	$\log k_6^c$
0.10	0.05	2.48	4.49	NC	3.23	4.33	NC	4.22	4.12	NC
	0.10	1.90	4.33	NC	2.43	4.21	NC	3.14	4.09	NC
	0.20	1.48	4.22	NC	1.79	4.15	NC	2.29	4.06	NC
	0.50	1.19	4.16	NC	1.33	4.13	NC	1.55	3.96	NC
	0.25	0.05	2.19	3.86	3.93	2.95	3.81	NC	4.13	3.73
0.25	0.10	1.85	3.88	NC	2.46	3.85	NC	3.38	3.80	NC
	0.20	1.53	3.88	NC	1.97	3.88	NC			
	0.50	1.21	3.81	NC	1.44	3.89	NC			
0.50	0.05	2.62	3.93	4.06	3.82	3.95	4.05	5.64	3.79	4.01
	0.10	2.40	4.05	NC	3.38	4.03	NC	4.93	3.89	3.99
	0.20	2.08	4.10	NC	2.91	4.10	NC	4.20	3.97	NC
1.00	0.05	2.46	3.50	3.68	3.56	3.53	3.68	5.66	3.51	3.82
	0.10	2.30	3.66	3.72	3.23	3.65	3.72	4.94	3.60	3.74
	0.20	2.06	3.77	NC	2.83	3.79	NC	4.17	3.71	NC
2.00	0.05	2.56	3.28	3.81	3.83	3.34	3.87	5.64	3.19	3.63
	0.10	2.49	3.52	3.72	3.61	3.53	3.73	5.11	3.31	3.59
	0.20	2.35	3.70	NC	3.29	3.67	3.72	4.53	3.46	3.65
4.00	0.05	2.32	2.77	3.25	3.46	2.89	3.35			
	0.10	2.34	3.10	3.35	3.32	3.11	3.35			
	0.20	2.26	3.32	3.42	3.11	3.31	3.40			

^aDMF with 0.1 M TBAPF₆ at 298 K. ^bValues determined assuming an ECE mechanism. ^cValues determined with inclusion of reaction 5; changes less than 0.05 were considered "no change", NC.

two molecules of **1** would consume two electrons to form one molecule of **5** and the n value would be exactly 1.0, compared to the 1.1–1.2 values observed (Table I).

Nitrocyclohexane (**6**) could be formed by protonation of nitronate **4**, but **4** is a weak base and there are no good proton donors present in the system. Indeed, the addition of water had little effect on the yield of **6** (Table I). A more likely source of **6** would be hydrogen atom abstraction by nitroalkyl radical **3**. Thinking that the solvent may be the hydrogen atom source, we replaced DMF with benzonitrile whose aromatic hydrogens are not easily removed. Again, there was little effect on the yield of **6** (Table I).

Indirect reduction was carried out by using 2-nitrobenzonitrile as redox catalyst; i.e., the more easily reduced 2-nitrobenzonitrile was reduced at the electrode to its anion radical, which in turn transferred an electron to **1**. The results are not notably different from those obtained by direct reduction. However, direct reduction in the presence of the radical inhibitor di-*tert*-butyl nitroxide^{7a} decreased the yield of dimer, produced substantial amounts of nitrocyclohexane, and left a significant residue of nitronate at the end of the electrolysis (Table I). Each of these observations is consistent with an intervention in the radical chain reaction that produces dimer **5**.

The total percentage of the carbon skeleton of **1** found in **5**, **4**, and **6** was never larger than 80%. Some of the missing material may be present as bicyclohexylidene, formed by reduction of **5**.^{3c} Fluctuations in the cathode potential could result in some reduction of **5** (cf. Figure 1), which would also account for the additional nitrite that was typically found and the larger-than-unity n values (Table I).

Homogeneous Redox Catalysis. The qualitative features of the cyclic voltammetry and the product analysis are suggestive of a reaction scheme that includes the rapid ECE reduction^{14a} of **1** (eqs 1–4) followed by a somewhat slower radical chain reaction to produce **5**. The lifetime of the radical anion **2** in the postulated ECE scheme must be very short as judged by the failure to detect it by fast-scan cyclic voltammetry.

We turned to homogeneous redox catalysis to study the first two steps of the postulated ECE scheme, eqs 1 and 2. The studies were conducted by cyclic voltammetry at a platinum disk electrode. The catalytic effect is illustrated in Figure 2 where the principal peak for reduction of **1** alone appears at -1.3 V. When catalyst **P** (2-methyl-1,4-naphthoquinone in this example) is studied alone, a reversible set of voltammetric peaks is seen corresponding to $P + e = Q$, Q being the anion radical of the quinone. Finally,

a mixture of **1** and **P** shows enhanced current at the potential where **P** is reduced. The excess current is due to the catalyzed reduction of **1** by homogeneous redox catalysis through the P/Q couple, eq 6, followed by reactions 2–4. The value of k_6 is much



smaller than the rate constant for electron transfer from **Q** to **3**, causing the reduction of **3** (eq 3) to be effected by solution electron transfer rather than direct electrode reaction.^{14d} A theoretical treatment of homogeneous redox catalysis as studied by cyclic voltammetry is available for the overall ECE reduction of a substrate.^{14c} The application of the technique requires acquisition of the peak currents, i_p , at a variety of scan rates for various concentrations of catalyst **P** and **1**. The quantity $i_p/2\gamma i_{pd}$ is calculated, and $\lambda_6 = k_6 C_P^*/(Fv/RT)$ is obtained by reference to theoretical working curves. Here $\gamma = C_1^*/C_P^*$, the ratio of bulk concentrations of substrate and catalyst, and i_{pd} is the cathodic peak current for reduction of the catalyst alone, other conditions being the same as used to obtain i_p . The theoretical working curves used assume that the forward electron-transfer rate, k_6 , controls the magnitude of i_p .

As demonstrated in studies of the direct reduction of **1** by cyclic voltammetry, the dimer **5** is formed in a subsequent reaction that probably consumes additional **1**. This feature is not included in the theoretical treatment of Andrieux et al.,^{14c} so we constructed modified working curves using digital simulation (as reported by Evans and Xie¹⁵) with inclusion of the reaction of **1** with **2** to give

(14) (a) The acronym ECE refers to an electrode reaction scheme comprising an electrochemical step (E) followed by a chemical step (C) that generates an easily reduced intermediate that reacts in a second electrochemical step (E). In the present case, these steps are eq 1 (E), eq 2 (C), and eq 3 (E). A pure ECE reaction involves only these three reactions. Specifically, the product of the C step is reduced directly at the electrode, eq 3. However, the easily reduced product of the C step can also be reduced by the product of the first E step via a solution electron-transfer (SET) reaction. In the present case, this reaction is eq 4. As anion radical **2** and radical **3** formally have the same oxidation state, this reaction is a type of disproportionation, giving an oxidized product (**1**) and a reduced product (**4**). Hence, this reaction scheme has been called DISP, specifically DISP1 when the rate-determining step is the first-order C step, eq 2.^{14b} Whether a reaction proceeds by pure ECE or DISP1 depends on the values of scan rate (v), rate constant (k_2) for the chemical step (which in our case is essentially irreversible), the rate constant for the SET reaction (k_4), and concentration of reactant (C_1^*). The regions of dominance of ECE or DISP1 are conveniently displayed in a kinetic zone diagram.^{14b} Put simply, increases in k_2 favor ECE while increases in k_4 , v , or C_1^* favor DISP1. (b) Amatore, C.; Savant, J.-M. *J. Electroanal. Chem.* 1977, 85, 27–46. (c) Andrieux, C. P.; Blocman, C.; Dumas-Bouchiat, J. M.; M'Halla, F.; Savant, J.-M. *J. Electroanal. Chem.* 1980, 113, 19–40. (d) Savant, J. M.; Su, K. B. *J. Electroanal. Chem.* 1985, 196, 1–22.

(13) Kornblum, N.; Boyd, S. D. *J. Am. Chem. Soc.* 1970, 92, 5784–5785.

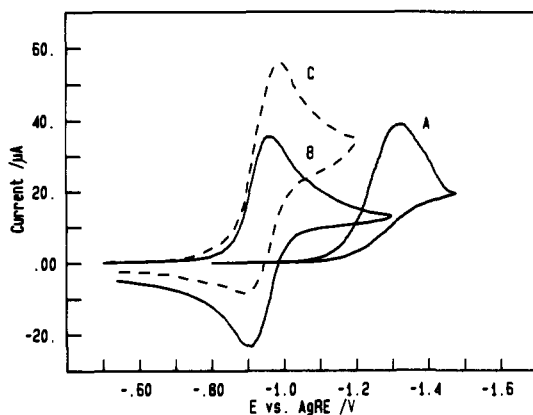


Figure 2. Homogeneous redox catalysis of the reduction of 1,1-dinitrocyclohexane in DMF with 0.10 M TBAPF₆ at 298 K. A 0.35-cm radius platinum disk working electrode. Scan rate 50 mV/s. (A) 0.50 mM 1,1-dinitrocyclohexane (1). (B) 0.50 mM 2-methyl-1,4-naphthoquinone (catalyst, P). (C) 0.50 mM 1 + 0.50 mM P.

5 and nitrite (eq 5) as a process first-order in each reactant. A value of $10^3 \text{ L mol}^{-1} \text{ s}^{-1}$ was used for k_5 . This value was determined by simulating cyclic voltammograms of the direct reduction of 1 assuming a two-electron reduction of 1 to 4 followed by the reaction of 1 and 4 (eq 5) to give dimer.

A typical set of data is given in Table II in which it may be seen that inclusion of this reaction narrows the range of the values of the evaluated rate constants and causes a significant increase in the average value of the rate constant, especially in cases where considerable catalysis has occurred as evidenced by large values of i_p/i_{pd} .

An examination of the data in Table II reveals a tendency for the calculated $\log k_6$ to decrease as C_P^* increases. This is especially evident for $C_P^* = 4.0 \text{ mM}$. The tendency indicates that i_p is not controlled solely by k_6 , but also the rate of the follow-up chemical reaction, eq 2, and the electron-back-transfer rate constant, k_{-6} , are influencing the current. This condition is known as "mixed control".¹⁴ Working curves of i_p/i_{pd} versus $\log(\lambda_2/\lambda_{-6})$ were constructed for given values of k_6 by using digital simulation as discussed above, where $\lambda_2 = k_2/(Fv/RT)$ and $\lambda_{-6} = k_{-6}C_P^*/(Fv/RT)$. Analysis of the data for 2-chloro-9,10-anthraquinone shows that when C_P^* is equal to or less than 0.5 mM, i_p is determined solely by k_6 . Therefore, the value of k_6 found for these catalyst concentrations (Table II) is the true value. With use of this value, the mixed-control working curves, and the data when C_P^* is greater than 0.5 mM, a value for $k_2/k_{-6} = 4.0 \times 10^{-4} \text{ mol/L}$ was found. This value should be independent of the identity of the catalyst since k_2 is independent of catalyst and k_{-6} is diffusion controlled (vide infra).

The data for even the lowest concentrations of the remaining catalysts were found to lie in the mixed-control regime and were analyzed by using the above value of k_2/k_{-6} to find k_6 . Table III gives the average value of k_6 for each of the catalysts as well as the range of γ and C_P^* in which the data could be analyzed according to the mixed-control working curves.

A plot of $\log k_6$ vs potential of the catalyst couple is presented in Figure 3, which includes earlier data obtained in DMSO by Bordwell and Bausch.¹⁶ These researchers determined rate constants for electron transfer to 1 from a series of substituted fluorenides. The fluorenides play the role of Q in eq 6. It was not possible to obtain a reversible response for oxidation of the fluorenides to the corresponding fluorenyl radicals, so the irreversible anodic peak potentials were measured and used by Bordwell and Bausch¹⁶ in the analysis of their data. These researchers argued that the irreversible peak potentials should be close to the reversible half-wave potential, and comparison of their data with the two values we obtained by redox catalysis (Table

Table III. Summary of 1,1-Dinitrocyclohexane Rate Constants^a

catalyst	E°_{PQ} (V)	$\log k_6$ ($\text{M}^{-1} \text{ s}^{-1}$)	C_P^* (mM)	γ
9,10-anthraquinone	-1.306	5.0 ± 0.2	1.0–2.0	0.5–2.0
2-chloro-9,10-anthraquinone	-1.214	4.0 ± 0.2	1.0–4.0	1.0–4.0
2-methyl-1,4-naphthoquinone	-1.161	3.3 ± 0.2	0.5–4.0	1.0–4.0
2,6-dimethoxy-1,4-benzoquinone	-1.139	2.9 ± 0.1	0.5–4.0	1.0–4.0
2,6-di- <i>tert</i> -butyl-1,4-benzoquinone	-1.106	2.4 ± 0.1	0.5–4.0	1.0–4.0
2,5-dimethyl-1,4-benzoquinone	-1.061	1.7 ± 0.2	0.5	4.0–16.0
2-methyl-1,4-naphthoquinone ^b	-1.090	3.19	1.0–4.0	1.0–4.0
2,6-dimethoxy-1,4-benzoquinone ^b	-1.068	2.72		

^aData obtained at 298 K with 0.10 M TBAPF₆ in DMF solvent unless otherwise specified. Potentials referred to ferricenium/ferrocene couple in the same solvent. In DMF, this potential is +0.051 V vs the AgRE used in this work. ^bDMSO as solvent.

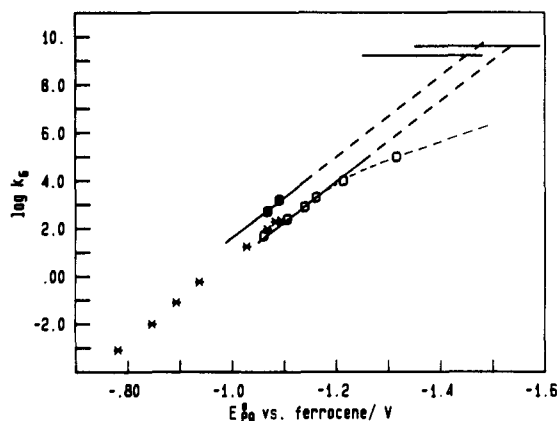


Figure 3. Rate constants for forward electron-transfer reaction 6. (O) Data obtained by homogeneous redox catalysis using quinone catalysts in DMF. (●) Homogeneous redox catalysis in DMSO. (*) Data obtained by using fluorenides as electron donors in DMSO.¹⁶ Estimated diffusion-controlled rate constants in DMF (upper) and DMSO (lower) indicated by horizontal lines. Extension of DMF data into activation-controlled region based on constructing a line through the anthraquinone point corresponding to a transfer coefficient of $1/2$ (see text).

III) in DMSO confirms their view. The irreversible peak potentials for oxidation of the fluorenides should be slightly negative of the reversible potentials due to the fast dimerization of the fluorenyl radicals following oxidation.¹⁷ The data in Figure 3 are consistent with an average of 55 mV for this negative displacement.

The slope of the plot is close to $-1/0.059 \text{ V}^{-1}$, which indicates¹⁸ that the rate constant for the reverse of reaction 6, k_{-6} , is constant for all the electron donors Q and that it is at the diffusion-controlled limit, k_{dif} . For the diffusion coefficients and sizes of the reactants P and 2, k_{dif} was estimated¹⁹ to be 4.0×10^9 and $1.6 \times 10^9 \text{ L mol}^{-1} \text{ s}^{-1}$ for DMF and DMSO, respectively. The extrapolated lines of $-1/0.059 \text{ V}^{-1}$ slope (Figure 3) should reach $\log k_{dif}$ at the reversible formal potential of eq 1, E_1° .¹⁸ The result for E_1° is -1.53 for DMF and -1.45 V for DMSO with respect to the reversible half-wave potential for ferricenium/ferrocene (in the same solvent).

Direct measurement of the formal potential for eq 1 would be quite difficult due to the short lifetime of the anion radical 2. The conclusion that the potential in DMSO is 80 mV positive of that

(15) Evans, D. H.; Xie, N. *J. Am. Chem. Soc.* **1983**, *105*, 315–320.

(16) Bordwell, F. G.; Bausch, M. J. *J. Am. Chem. Soc.* **1986**, *108*, 1985–1988.

(17) Olmstead, M. L.; Hamilton, R. G.; Nicholson, R. S. *Anal. Chem.* **1969**, *41*, 260–267.

(18) Andrieux, C. P.; Blocman, C.; Dumas-Bouchiat, J. M.; Savéant, J.-M. *J. Am. Chem. Soc.* **1979**, *101*, 3431–3441.

(19) Kojima, H.; Bard, A. J. *J. Am. Chem. Soc.* **1975**, *97*, 6317–6324.

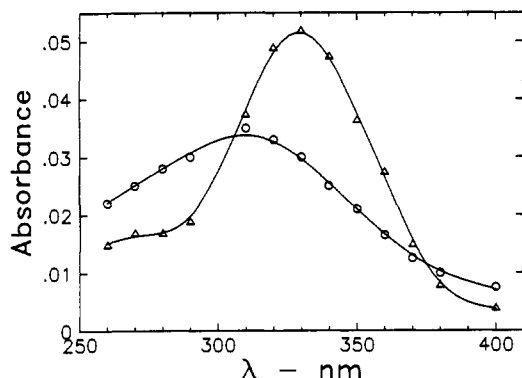


Figure 4. Optical absorption spectra at various times after pulse radiolysis of 0.5 mM 1,1-dinitrocyclohexane in 1/4 *tert*-butyl alcohol-water (V/V) with 2 mM pH 7 phosphate buffer. Monitored 1 μ s (O) and 7 μ s (Δ) after the pulse.

in DMF is consistent with measurements of reversible potentials for substituted nitrobenzenes.²⁰ The difference is attributable to stronger solvation of the anion radical by DMSO as compared to DMF.

Finally, the value of $k_2/k_{-6} = 4.0 \times 10^{-4}$ mol/L, evaluated above for DMF, can be combined with $k_{\text{dir}} = k_{-6} = 4.0 \times 10^9$ L mol⁻¹ s⁻¹ to obtain $k_2 = 1.6 \times 10^6$ s⁻¹.

Pulse Radiolysis. A different method of generating radical anion **2** and monitoring its decay is needed to test the validity of the results of homogeneous redox catalysis. Pulse radiolysis of aqueous solutions provides a means of generating strongly reducing species (principally the hydrated electron) on the nanosecond time scale. The hydrated electrons rapidly reduce electron acceptors, producing a population of anion radicals within a short period. The formation and reaction of the anion radicals can be monitored by UV-visible absorption spectrophotometry in the microsecond time scale.

When **1** was investigated in 20% *tert*-butyl alcohol and 80% water, at pH 7, a rapid increase in absorbance was observed with a maximum near 310 nm (Figure 4). This peak was assigned to the radical anion **2**. The absorbance at 270–290 nm decayed with a rate constant of $(1.1 \pm 0.4) \times 10^6$ s⁻¹. Concurrent with this decay was an increase in absorbance centered around 330 nm (Figure 4). Analysis of this buildup gave rate constants consistent with the decay of the 290 peak but less precise due to interference by earlier and later processes. The 330-nm band was assigned to nitroalkyl radical **3**. Similar spectra and rate constants were observed in the absence of *tert*-butyl alcohol and also when *tert*-butyl alcohol was replaced by isopropyl alcohol. Thus, in aqueous media, the value of k_2 is about 1.1×10^6 s⁻¹ compared to 1.6×10^6 s⁻¹ found in DMF by homogeneous redox catalysis. In view of the precision of the measurements, these values are regarded as identical.

Support for the assignment of the 330-nm band to **3** was found in pulse radiolysis of the nitronate anion **4**. Pulse radiolysis of bromide-containing solutions saturated with N₂O produces the strong oxidant Br₂^{•+}.²¹ When an aqueous solution of nitrocyclohexane, 0.5 M KBr, and 0.03 M KOH was studied, Br₂^{•+} ($\lambda_{\text{max}} = 360$ nm) formed promptly followed by a species giving a band centered at about 330 nm, which is assigned to nitroalkyl radical **3** formed by oxidation of nitronate **4** by Br₂^{•+} (Figure 5). The absorbance at 330 nm slowly decays to give a species that absorbs below 300 nm. Presumably, **3** reacts with excess nitronate to give the anion radical **7** of 1,1'-dinitrobicyclohexyl, eq 7. When the pseudo-first-order decay of **3** was studied as a function of the concentration of nitronate, a linear relation was found between the pseudo-first-order rate constant and concentration. The slope gave $k_7 = (2.6 \pm 0.9) \times 10^6$ L mol⁻¹ s⁻¹. The intercept of the

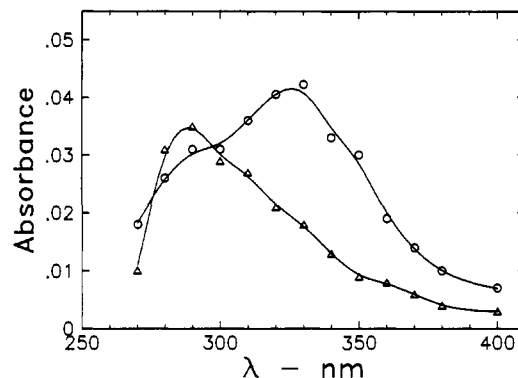


Figure 5. Differential absorption spectra after pulse radiolysis of 3 mM nitrocyclohexane in 0.5 M aqueous KBr with 0.03 M KOH. Monitored 6 μ s (O) and 24 μ s (Δ) after the pulse.

plot was relatively high (1.1×10^5 s⁻¹) due to radical-radical reactions competing with reaction 7.

Discussion

First Step of Reduction, Equation 1. The studies by homogeneous redox catalysis have provided new information about the reduction of **1** to its anion radical. The value of E_1° for reduction of 1,1-dinitrocyclohexane, -1.53 V in DMF, is a reflection of the strong anion stabilization brought about by the *gem*-dinitro group. By contrast, the reversible half-wave potential for reduction of nitrocyclohexane is -2.28 V while that of the *vic*-dinitro compound 1,1'-dinitrobicyclohexyl is -2.08 V, with all potentials referred to the reversible ferricenium/ferrocene couple in DMF.^{3c}

Electron transfer to aliphatic nitro compounds is somewhat sluggish, both in solution and at an electrode-solution interface.^{11,22} If that is the case for 1,1-dinitrocyclohexane, the values of k_6 in Figure 3 will not increase as rapidly as the linear extrapolation would predict as catalyst couples with potentials very close to E_1° are used. The data are then in a region of "activation control".¹⁸ Only one catalyst, anthraquinone, falls in this region. The line corresponding to a transfer coefficient of 0.5 was constructed through the anthraquinone point to provide a rough estimate of the value of k_6 at zero driving force (i.e., for a hypothetical quinone catalyst whose standard potential equals E_1°). The result is $\log k_6 = 6.7$.

The "cross relation"²³ gives this rate constant in terms of the self-exchange rate constants for the quinone and 1,1-dinitrocyclohexane neutral/anion radical, k_{11} and k_{22} , respectively.

$$k_6 = (k_{11}k_{22})^{1/2}$$

Self-exchange rate constants for 1,4-benzoquinone and 1,4-naphthoquinone in DMF average 4.6×10^8 L mol⁻¹ s⁻¹.²⁴ Using this value for k_{11} and 5×10^6 L mol⁻¹ s⁻¹ for k_6 (vide supra) gives k_{22} , the self-exchange rate constant for **1/2**, equal to about 5×10^4 L mol⁻¹ s⁻¹. For comparison, the self-exchange rate constant for *tert*-nitrobutane and its anion radical in acetonitrile is 5×10^3 L mol⁻¹ s⁻¹.¹⁴ Of course, this exercise should not be regarded as a serious attempt to determine the self-exchange rate constant for 1,1-dinitrocyclohexane. Rather, its purpose is to show that the data are consistent with the expectation that a somewhat suppressed rate pertains for this nitroalkane just as is seen with others.

(22) (a) Peover, M. E.; Powell, J. S. *J. Electroanal. Chem.* **1969**, *20*, 427–433. (b) VandenBorn, H. W.; Evans, D. H. *Anal. Chem.* **1974**, *46*, 643–646. (c) Savéant, J.-M.; Tessier, D. *J. Electroanal. Chem.* **1975**, *65*, 57–66. (d) Savéant, J.-M.; Tessier, D. *J. Phys. Chem.* **1977**, *81*, 2192–2197. (e) Corrigan, D. A.; Evans, D. H. *J. Electroanal. Chem.* **1980**, *106*, 287–304. (f) Amatore, C. A.; Savéant, J.-M.; Tessier, D. *J. Electroanal. Chem.* **1983**, *146*, 37–45. (g) Petersen, R. A.; Evans, D. H. *J. Electroanal. Chem.* **1987**, *222*, 129–150.

(23) Marcus, R. A.; Sutin, N. *Biochim. Biophys. Acta* **1985**, *811*, 265–322.

(24) Malachuk, P. A.; Miller, T. A.; Layloff, T.; Adams, R. N. *Exch. React., Proc. Symp.* **1965**, 157–171.

(20) Shalev, H.; Evans, D. H. *J. Am. Chem. Soc.* **1989**, *111*, 2667–2674.

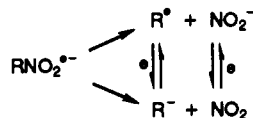
(21) (a) Jayson, G. G.; Parsons, B. J.; Swallow, A. J. *J. Chem. Soc., Faraday Trans. 1* **1973**, *69*, 1597–1607. (b) Schwartz, H. A.; Dodson, R. W. *J. Phys. Chem.* **1984**, *88*, 3643–3647.

Cleavage of Nitrite from 2, Equation 2. Both homogeneous redox catalysis and pulse radiolysis give a value of about 10^6 s^{-1} for the rate constant for this process. For comparison, rate constants for loss of nitrite from the anion radicals of mononitro compounds are of the order of 1 s^{-1} and those of *vic*-dinitro compounds are of the order of 10^3 s^{-1} .³ Obviously, the α -nitro substituent in **1** has a very strong activating effect on this cleavage reaction.

The cleavage reaction, eq 2, is a key step in the ECE-type reduction of **1**. The initial electron-transfer reaction (E), eq 1, is followed by this very fast chemical step (C), producing nitrite and nitroalkyl radical **3**. This radical is very easily reduced as the potential for the radical/nitronate anion couple, $3 + e = 4$, must be quite positive as indicated by the irreversible oxidation process for **3** seen at about -0.25 V vs AgRE. This potential is consistent with oxidation of other nitronates.²⁵ Thus, there is a large driving force for reduction of **3**, either at the electrode, eq 3 (ECE), or by the anion radical **2**, eq 4 (DISP1).

It is interesting to see whether ECE or DISP1 conditions^{14a} pertain in this reaction. Taking the forward rate constant of eq 4 to be diffusion controlled (due to the large driving force) and using $k_2 = 10^6 \text{ s}^{-1}$, the kinetic zone diagram^{14b} shows that the system is in the DISP1 region for any scan rate exceeding about 0.1 V/s . Thus, under most of the conditions employed, nitroalkyl radical **3** is reduced principally by reaction with **2** (DISP1) rather than directly at the electrode surface (ECE). This arises because the lifetime of **2**, though brief, is sufficient for it to diffuse away from the electrode surface before cleavage occurs.

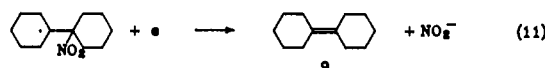
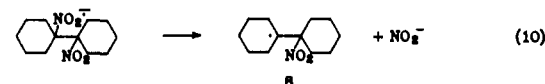
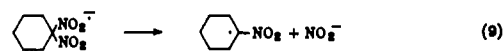
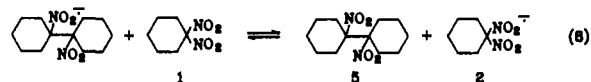
In principle, the anion radical of a nitro compound could cleave to give NO_2 and a carbanion. In the present case, the reaction would be $2 \rightarrow 4 + \text{NO}_2$. Whether NO_2 or nitrite is lost depends mainly upon the relative potentials of the $\text{NO}_2/\text{nitrite}$ ($E^\circ_{\text{NO}_2/\text{NO}_2^-}$) couple and the radical/carbanion ($E^\circ_{\text{R}\cdot/\text{R}^-}$) couple. When



$E^\circ_{\text{NO}_2/\text{NO}_2^-}$ is more positive than $E^\circ_{\text{R}\cdot/\text{R}^-}$, nitrite will be lost just as was observed for **2**. The opposite behavior is known for tetranitromethane, which by pulse radiolysis gives trinitromethanide anion and NO_2 , reflecting the very positive potential of the trinitromethyl radical/trinitromethanide couple.²⁶ Interestingly, *gem*-dinitro compounds are probably close to a transitional stage, the irreversible oxidation potential of the anion **4** being only about $0.3\text{--}0.5 \text{ V}$ less positive than that of nitrite.

Subsequent Reaction of Nitronate with 1 To Give 5. The DISP1 mechanism, given by eqs 1–4, is followed by what is formally a "father-son" reaction²⁷ in which nitronate **4** reacts with starting material **1** to give the dimer **5** and nitrite (eq 5). On the surface, this reaction would appear to be the simple nucleophilic displacement of nitrite by the nitronate anion, but it is known that it proceeds by a radical chain reaction.⁷ Though the detailed kinetics of these reactions have not been elucidated, it is thought that the initiation reaction is electron transfer between **4** and **1** to give **2** and **3**. The chain-carrying steps would be eqs 7–9 (Scheme II) (eq 9 is the same as eq 2 given earlier) with various termination steps possible such as hydrogen atom abstraction by **3** to give nitrocyclohexane, dimerization of **3**, and in our case, the known loss of nitrite from anion radical **7** (eq 10) followed by reduction (eq 11).^{3c} The overall process is much slower than the

Scheme II



cleavage of nitrite from radical anion **2**, and it was possible to outrun it with fast-scan cyclic voltammetry (*vide supra*).

Initiation of the reaction in the electrochemical context differs from that with no electrode present. As stated above, the initiation is thought to involve electron transfer from **4** to **1**, giving **3** and **2**, a reaction that is energetically unfavorable by over 1 eV . When the reaction occurs during reduction of **1** at an electrode, the key nitroalkyl radical intermediate **3** is being generated in the DISP1 reduction so an alternate initiation path is operative.

An unanticipated benefit of the studies by pulse radiolysis was the determination of the rate constant for addition of nitroalkyl radical **3** to nitronate **4** (eq 7). This is a key step in the radical chain reaction, and its rate appears to be large enough to support a relatively rapid process.

We thought that a significant test of these ideas would be to attempt to accommodate the cyclic voltammetric data by the complex reaction scheme of the DISP1 (eqs 1–4) followed by the radical chain reaction (eqs 7–9) with termination by eqs 10 and 11. The principal interest was to predict the amount of dimer **5** produced, as reflected in its reduction peak near -2.0 V (Figure 1), for a variety of scan rates and concentrations of **1**.

In such a complex reaction scheme, it is highly desirable to reduce the number of adjustable parameters to an absolute minimum. Fortunately, many of the parameters are known or can be reliably estimated. Thus, the standard potential for eq 1 and the rate constant for eq 2 were measured in earlier stages of this work. As has been argued earlier, the rates of eqs 3 and 4 should be near the diffusion-controlled limit. Hence, the surface concentration of **3** was maintained at zero, and k_4 was set equal to $10^{10} \text{ L mol}^{-1} \text{ s}^{-1}$. The equilibrium constant for eq 8 is 10^6 based on the standard potentials for eq 1 and that for reduction of **5** to its radical anion **7**.^{3c} Reaction 8 may be sufficiently downhill to occur near the diffusion-controlled rate. A somewhat smaller value was selected, $k_8 = 10^9 \text{ L mol}^{-1} \text{ s}^{-1}$. Independent measurements^{3c} of the loss of nitrite from **7** (eq 10) give $k_{10} = 6 \times 10^3 \text{ s}^{-1}$ at 298 K . Finally, the nitroalkyl radical **8** is readily reduced, so its surface concentration was held at zero.

One adjustable chemical kinetic parameter remains, *viz.*, rate constant k_7 .²⁸ When the value of $k_7 = 2.6 \times 10^6 \text{ L mol}^{-1} \text{ s}^{-1}$ (found by pulse radiolysis) was used, the simulations²⁹ showed no peak for reduction of dimer **5** under conditions where it was plainly evident in the experimental voltammogram. In other words, the radical chain reaction (eqs 7–9) with this value of k_7 is simply not efficient enough to produce the observed yield of **5**. An

(25) (a) Schäfer, H. *Chem.-Ing.-Tech.* **1969**, *41*, 179–185. (b) Wawzonek, S.; Su, T.-Y. *J. Electrochem. Soc.* **1973**, *120*, 745–747.

(26) (a) Asmus, K.-D.; Henglein, A.; Ebert, M.; Keen, J. P. *Ber. Bunsen-Ges. Phys. Chem.* **1964**, *68*, 657–663. (b) Rabani, J.; Mulac, W. A.; Matheson, M. S. *J. Phys. Chem.* **1965**, *69*, 53–70.

(27) (a) Elving, P. J. *Can. J. Chem.* **1977**, *55*, 3392–3412. (b) Amatore, C.; Capobianco, G.; Farnia, G.; Sandonà, G.; Savéant, J.-M.; Severin, M. G.; Vianello, E. *J. Am. Chem. Soc.* **1985**, *107*, 1815–1824. (c) In view of the somewhat indirect relationship between family members **1** and **4**, the father-son reaction^{27a} might better be called a "grandfather-grandson"^{27b} or even "uncle-nephew" reaction.

(28) The other parameters are the heterogeneous electron-transfer rate constants and transfer coefficients of eq 1 and the 5/7 couple. In practice, these were adjusted to reproduce the shape and position of the two reduction peaks. The simulated currents were scaled to match experimental at the first reduction peak. Simulations were terminated at potentials preceding those needed for the second step of reduction of **5** or reduction of nitrocyclohexane.^{3c}

(29) Feldberg, S. W. In *Electroanalytical Chemistry. A Series of Advances*; Bard, A. J., Ed.; Marcel Dekker: New York, 1969; Vol. 3, pp 199–296.

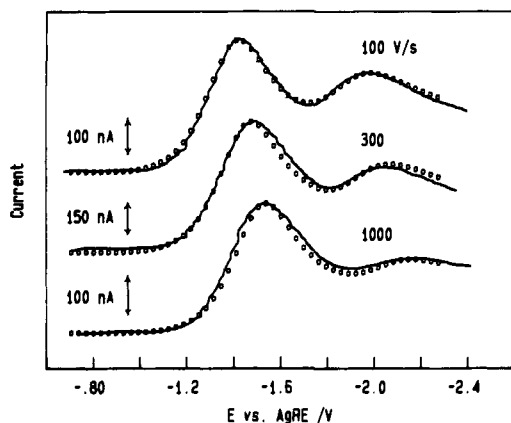


Figure 6. Comparison of digital simulations (points) with cyclic voltammograms (full curves) for 2.4 mM **1**. A 50- μm diameter platinum disk for 100 and 300 V/s; 25 μm for 1000 V/s. Simulation parameters: $E^{\circ}_1 - E^{\circ}_{12} = 0.35$ V; $\alpha_1 = 0.3$; $\alpha_{12} = 0.2$; $k_{s,1} = k_{s,12} = 0.01$ cm/s; $k_2 = 2 \times 10^6$ s $^{-1}$; $k_7 = 4.7 \times 10^8$ L mol $^{-1}$ s $^{-1}$; other values in text. Reaction numbers referred to by subscripts; reaction 12 is **5** + e = **7**.

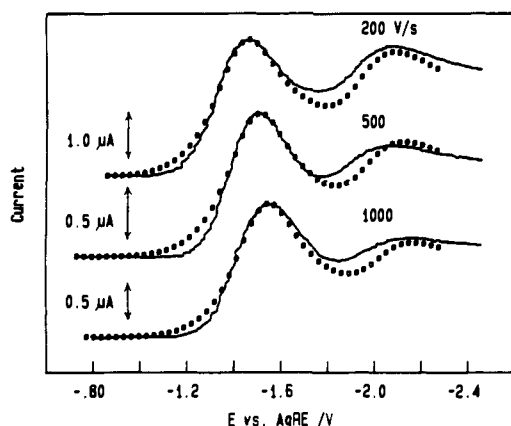


Figure 7. Comparison of digital simulations (points) with cyclic voltammograms (full curves) for 15 mM **1**. A 50- μm diameter platinum disk for 200 V/s; 25 μm for 500 and 1000 V/s. Same simulation parameters as in Figure 6.

increase of about 2 orders of magnitude in the rate constant of eq 7 was needed to generate peaks for reduction of **5** resembling those seen experimentally.

For the slower scan rates, these simulations predicted that more **5** was formed than was found in the voltammograms. Recalling that nitrocyclohexane (**6**) was always found among the products

of electrolysis (Table I), we introduced the additional termination reaction, hydrogen atom abstraction by nitroalkyl radical **3** to give nitrocyclohexane in a pseudo-first-order reaction with rate constant k_t . Comparison of simulation and experiment is illustrated in Figure 6 for three scan rates between 100 and 1000 V/s and 2.4 mM **1**. Now, with inclusion of hydrogen atom abstraction ($k_t = 2 \times 10^4$ s $^{-1}$), the variation in the relative heights of the two peaks with scan rate is adequately accounted for by the scheme. Similar agreement between simulation and experiment was found for a total of six scan rates in the range of 100–1000 V/s. All simulation parameters were maintained constant in the series of simulations.

There are several important second-order reactions in the scheme, particularly reaction 7. Hence, it is expected that relatively more **5** will be formed when the concentration of reactant **1** is increased. Results for 15 mM **1** are shown in Figure 7. The values for all simulation parameters were the same as those used to match the 2.4 mM results. Though the agreement is not as good as found for the lower concentration, the simulations do account for the relatively larger peak height for reduction of **5** and its variation with scan rate. The poor agreement seen in the valley region between the reduction peaks suggests that a significant process has been ignored in the scheme, perhaps adsorption of reaction intermediates.

In view of the various approximations introduced in the simulations, the value of $k_7 = 4.7 \times 10^8$ L mol $^{-1}$ s $^{-1}$ for DMF cannot be considered to be exact. Nevertheless, the rate constant is clearly larger than seen in water by pulse radiolysis, $k_7 = 2.6 \times 10^6$ L mol $^{-1}$ s $^{-1}$. Rates of reactions of anions are often much larger in dipolar aprotic solvents than in water,³⁰ an observation related to the unusually poor solvation of anions by solvents such as DMF. From the simulations, it was learned that a value as small as 10^6 L mol $^{-1}$ s $^{-1}$ would not produce enough **5** to detect a peak for its reduction at 100 V/s. This suggested the following test: If the rate of reaction 7 is 100 times slower in water than DMF, cyclic voltammograms obtained in water will show no peak for the reduction of **5**. When 2.7 and 5.3 mM **1** was studied in an aqueous solution of 0.30 M tetraethylammonium bromide at a hanging mercury drop electrode, no unambiguous peak for **5** could be found even at scan rates as low as 1 V/s, thus confirming the substantial solvent effect on the rate of reaction 7.

Acknowledgment. This research was supported by the National Science Foundation, Grant CHE9100281. J.C.R. was supported by a National Science Foundation Graduate Fellowship. The pulse radiolysis studies at NIST were supported by the Office of Basic Energy Sciences of the Department of Energy.

(30) Reichardt, C. *Solvents and Solvent Effects in Organic Chemistry*, 2nd ed.; VCH: Weinheim, 1988; pp 121–283.